The stress field of an infinite set of discrete dislocations

Sivasambu Mahesh[a], Shyam M. Keralavarma[a]

[a]Department of Aerospace Engineering, Indian Institute of Technology Madras, Chennai 600036. India.

ARTICLE HISTORY
Compiled March 13, 2021

ABSTRACT
The two-dimensional stress fields induced by a set of infinitely many parallel edge dislocations are difficult to estimate as those of individual dislocations decay slowly. A simple numerical method to compute them is proposed. The method is based on series summation using a convergence factor, $\exp(-sr^2)$ that decays rapidly with radial distance r from the field point, and letting the positive parameter $s \downarrow 0$ numerically through Richardson extrapolation. The present method is more general than a lattice summation method with explicit spurious stress cancellation that is widely used in the literature. Furthermore, the spurious long-range stresses are cancelled in the present method without explicit evaluation.

KEYWORDS
Dislocation, series summation, spurious stress, numerical method.

1. Introduction

Dislocation dynamics simulations have for long been used to bridge the atomistic and continuum length-scales [1, 2]. These simulations can be performed in two or three dimensions. While three dimensional simulations are more realistic, they are computationally tractable only under simple boundary conditions. Two dimensional discrete dislocation dynamics is still widely used to study complex boundary value problems involving free boundaries and internal interfaces, such as the deformation of thin films [3], growth of cracks and voids [4], and thermally activated plasticity at elevated temperatures [5, 6]. Although the physics of dislocation interactions is highly idealised in two dimensions, the relative efficiency of the method allows the simulation of large dislocation densities and image stresses due to free boundaries using commodity hardware, as opposed to large computing clusters needed for three-dimensional dislocation dynamics simulations.

The most computationally intensive part of dislocation dynamics simulations is the calculation of the resolved shear stresses at all the dislocation segments due to their mutual interaction [1, 7]. Two methods for performing this computation efficiently are the fast multipole method [8, 9], and the particle-in-cell method [10, 11]. In three-dimensional simulations, wherein the number of interacting slip systems is large, and mixed dislocation segments are typical, the former method is faster, and yields computer memory efficient implementations. Therefore, it has been implemented in a number of three-dimensional dislocation dynamics codes [7]. In two-dimensional dislocations

CONTACT S. Mahesh. Email: smahesh@iitm.ac.in

dynamics, however, the number of interacting slip systems seldom exceeds three. In this case, the particle-in-cell method is the faster, and more memory efficient method [11].

Two-dimensional dislocation dynamics simulations are performed in a simulation cell that lies in a plane normal to the common line direction of a set of dislocations. The dislocations are regarded as points in the normal plane. In the two-dimensional particle-in-cell method [10], the simulation cell is overlaid with a regular mesh. The method works with a continuous dislocation density function derived from the discrete distribution. Under periodic boundary conditions, the interaction forces between mesh elements can be computed efficiently in Fourier space. The mesh forces are then interpolated to obtain the resolved shear stresses at the individual dislocations.

As input, the particle-in-cell method requires the resolved shear stresses induced by a dislocation and its infinitely many periodic images, at the centres of the mesh elements [12]. However, this computation is not straightforward because the resolved shear stress field due to a dislocation decays slowly as the reciprocal of the distance from the dislocation, r [13]. The gradual decay makes neglecting all but a finite number of image dislocations inadmissible. A number of works [9, 14–16], have used an ingenious method to obtain the stress fields without such truncation, which is summarised in Sec. 2.3. This method is based on superposing the stress fields of one-dimensional arrays of dislocations [13]. Kuykendall and Cai [15] showed the importance of deducting linearly varying 'spurious' stress components to obtain a unique solution. Gourgiotis and Stupkiewicz [16] showed that the spurious stresses arise from the eigenstrain associated with the dislocations within the truncated domain.

In the sequel, a numerical procedure is developed to determine the stress fields induced by a set of infinitely many discrete edge dislocations. The periodic lattice of source dislocations, discussed above, is a special case of this general problem. The central idea of the present method is to modify the contribution of each image dislocation by a convergence factor, $\exp(-sr^2)$, which renders the infinite sum for the stress fields absolutely convergent. Evaluating the absolutely convergent sums for various positive s, and taking the limit as $s \downarrow 0$ yields an accurate estimate of the stress fields. It will be shown that the stress fields thus obtained are immune to spurious components.

2. Numerical method

2.1. Stress fields due to a set of dislocations

Consider an infinite set $\mathscr{I}$ of discrete straight edge dislocations, each with with line direction parallel to the z-axis, and with Burgers vector $b_{\mathrm{x}}\boldsymbol{e}_{\mathrm{x}} + b_{\mathrm{y}}\boldsymbol{e}_{\mathrm{y}}$. Here, $\boldsymbol{e}_{\mathrm{x}}$, and $\boldsymbol{e}_{\mathrm{y}}$ denote unit vectors along the x, and y-axes respectively. Let the i-th dislocation be located at (x_i, y_i). Let (x_i, y_i), $i \in \mathscr{I}$ be such that the number of dislocations in area A scales as $O(A)$ as $A \uparrow \infty$. Two examples that satisfy this condition are shown in Fig. 1.

The in-plane Volterra stress components at (x, y) due to an edge dislocation at the origin are [13]:

$$\begin{aligned}
\sigma^O_{xx}(x,y) &= (\kappa/\pi)\left\{-b_{\mathrm{x}}y(3x^2+y^2) + b_{\mathrm{y}}x(x^2-y^2)\right\}/(x^2+y^2)^2, \\
\sigma^O_{yy}(x,y) &= (\kappa/\pi)\left\{b_{\mathrm{x}}y(x^2-y^2) + b_{\mathrm{y}}x(x^2+3y^2)\right\}/(x^2+y^2)^2, \text{ and} \\
\sigma^O_{xy}(x,y) &= (\kappa/\pi)\left\{b_{\mathrm{x}}x(x^2-y^2) + b_{\mathrm{y}}y(x^2-y^2)\right\}/(x^2+y^2)^2,
\end{aligned} \tag{1}$$

where $\kappa = \mu/2(1-\nu)$, and where μ and ν denote the shear modulus and Poisson's ratio

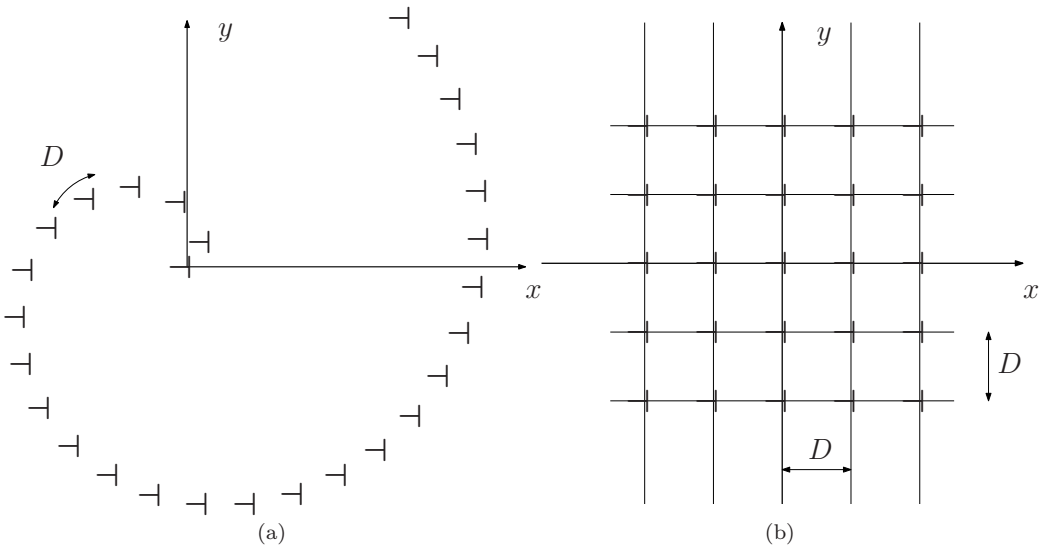

Figure 1. Two examples of infinite sets of discrete dislocations. (a) Dislocations arranged on a spiral with equal arc-wise spacing D, and (b) a square lattice of dislocations with lattice constant D.

of the isotropic material, respectively.

Consider a slip system with slip direction $\sin\theta\boldsymbol{e}_{\mathrm{x}} + \cos\theta\boldsymbol{e}_{\mathrm{y}}$, and slip plane normal $-\cos\theta\boldsymbol{e}_{\mathrm{x}} + \sin\theta\boldsymbol{e}_{\mathrm{y}}$. The Schmid tensor components in the xy coordinate system are [13]:

$$\begin{pmatrix} S_{xx} & S_{xy} \\ S_{xy} & S_{yy} \end{pmatrix} = -\frac{1}{2}\begin{pmatrix} \sin 2\theta & \cos 2\theta \\ \cos 2\theta & -\sin 2\theta \end{pmatrix}. \tag{2}$$

The relevant function of the stress field that governs dislocation motion by slip is the resolved shear stress, $\tau^O(x,y)$ [13]:

$$\tau^O(x,y) = \sigma^O_{xx}(x,y)S_{xx} + \sigma^O_{yy}(x,y)S_{yy} + 2\sigma^O_{xy}(x,y)S_{xy}. \tag{3}$$

The resolved shear stress at (x,y) due to all the dislocations in $\mathscr{I}$ can be obtained by superposing the individual contributions:

$$\tau(x,y) = \sum_{i\in\mathscr{I}} \tau^O(x-x_i, y-y_i). \tag{4}$$

Let the Euclidean distance of the field point (x,y) from dislocation $i \in \mathscr{I}$ be r_i. Let

$$\tau(x,y;R) = \sum_{\{i\in\mathscr{I}:r_i\le R\}} \tau^O(x-x_i, y-y_i). \tag{5}$$

Then, Eq. (4) may be written as $\tau(x,y) = \lim_{R\to\infty}\tau(x,y;R)$. However, $\tau(x,y;R)$ does not estimate $\tau(x,y)$ well for any finite R because σ^O_{ij} does not decay rapidly with r_i. This will be demonstrated in Sec. 3.

2.2. Convergence factor

The present use of a convergence factor to obtain a numerical estimate of $\tau(x, y)$ follows de Leeuw et al. [17], who used this method to sum a conditionally convergent series representing the Hamiltonian of a lattice of electrostatic charges. As the potential of a point charge is isotropic, de Leeuw et al. [17] could obtain an analytical expression for the series sum. However, as the anisotropic resolved stress field of a dislocation is not amenable to analytical summation, the present treatment is numerical.

Presently, the terms of Eq. (4) are modified by the convergence factor $\exp(-sr_i^2)$:

$$\tau(x, y; s) = \sum_{i \in \mathscr{I}} \tau^O(x - x_i, y - y_i) \exp(-sr_i^2), \tag{6}$$

where $s > 0$ is the convergence parameter. The convergence factor renders the sum Eq. (6) absolutely convergent. This is seen by recalling that σ_{ij}^O, and therefore, τ^O, decay as $O(1/r)$ with distance from the source dislocation. Consider an annulus of width dr at radius r from the field point (x, y). By assumption, the number of source dislocations within this annulus scales with its area, i.e., as $O(r)dr$. Therefore, the sum of the absolute values of all the terms in Eq. (6) with $r_i > R$ is of the order of $\int_R^\infty \exp(-sr^2) r(1/r) dr \approx \operatorname{erfc}(\sqrt{s}R)/\sqrt{s}$, which decays exponentially fast. $\operatorname{erfc}(\cdot)$ here denotes the complementary error function.

Requiring that the contribution of all the neglected summands in Eq. (6) be smaller than a prescribed tolerance, $\varepsilon > 0$, yields an expression for the cut-off radius:

$$R(s) = \frac{1}{\sqrt{s}} \operatorname{erfc}^{-1}(\sqrt{s}\varepsilon). \tag{7}$$

Thus, to $O(\varepsilon)$ accuracy, the resolved shear stress may be expressed as:

$$\tau(x, y; s) = \sum_{\{i \in \mathscr{I} : r_i \leq R(s)\}} \tau(x - x_i, y - y_i) \exp(-sr_i^2). \tag{8}$$

The limiting value, $\tau^*(x, y) = \lim_{s \downarrow 0} \tau(x, y; s)$, can be obtained using Richardson extrapolation [18], as follows. Let

$$\tau(x, y; s) = \tau^*(x, y) + cs^p + O(s^{p+1}), \tag{9}$$

where c is an unknown constant, and p denotes the rate-of-convergence exponent. p can be estimated from $\tau(x, y; s)$, $\tau(x, y; s/2)$, and $\tau(x, y; s/4)$ as [19]:

$$p \approx \log_2((\tau(x, y; s) - \tau(x, y; s/2))/(\tau(x, y; s/2) - \tau(x, y; s/4))). \tag{10}$$

$p > 0$, and $p < 0$ signify convergence, and divergence, respectively. Given $\tau(x, y; s)$, $\tau(x, y; s/2)$, and $p > 0$, Richardson's extrapolation [19, Chap. 7] estimates $\tau^*(x, y)$ as:

$$\tau^*(x, y) = \frac{2^p \tau(x, y; s/2) - \tau(x, y; s)}{2^p - 1} + O(s^{p+1}). \tag{11}$$

2.3. Array summation

The array summation approach used in the literature [9, 14–16] to obtain the stress fields due to the dislocation lattice shown in Fig. 1 (b) is now summarised. Let $\boldsymbol{\sigma}^{\text{array}}(x, y; m)$ denote the stress due to an array of dislocations parallel to the y-axis at $x = mD$, $m \in \{\ldots, -2, -1, 0, 1, 2, \ldots\}$ with dislocation spacing D. Closed form expressions for the stress components induced at (x, y) are given in Hirth and Lothe [13, Sec. 19.6] as:

$$\begin{aligned}
\sigma_{xy}^{\text{array}}(x, y; m) &= \sigma_0 \left(b_{\text{x}} X \left(\cosh X \cos Y - 1\right) - b_{\text{y}} \sin Y (\cosh X - \cos Y - X \sinh X)\right); \\
\sigma_{xx}^{\text{array}}(x, y; m) &= \sigma_0 \left(-b_{\text{x}} \sin Y (\cosh X - \cos Y + X \sinh X) + b_{\text{y}} X (\cosh X \cos Y - 1)\right); \text{ and} \\
\sigma_{yy}^{\text{array}}(x, y; m) &= \sigma_0 \left(-b_{\text{x}} \sin Y (\cosh X - \cos Y - X \sinh X) + \right. \\
&\qquad \left. b_{\text{y}} (2 \sinh X (\cosh X - \cos Y) - X (\cosh X \cos Y - 1))\right),
\end{aligned} \tag{12}$$

where $\sigma_0 = \kappa/(D(\cosh X - \cos Y)^2)$, $X = 2\pi(x - mD)/D$, and $Y = 2\pi y/D$. Correspondingly, $\tau^{\text{array}}(x, y; m)$, can be obtained by replacing σ^O in Eq. (3) with σ^{array}.

Summation of contributions $\tau^{\text{array}}(x, y; m)$ from the dislocation arrays yields the resolved shear stress, $\tau(x, y)$, induced by the square lattice. However, this sum suffers from spurious stress components. Kuykendall and Cai have determined explicit formulae [15, Eqs. (46), and (51)] for the spurious components, which must be deducted from the direct sum. For the dislocation arrangement of Fig. 1 (b) the corrected sum is:

$$\tau(x, y) = \lim_{N_c \to \infty} \sum_{m=-N_c}^{N_c} \tau^{\text{array}}(x, y; m) - 4\kappa \frac{b_{\text{y}}}{D} \frac{x}{D} S_{yy}. \tag{13}$$

As the short-range part of $\tau^{\text{array}}(x, y; m)$ decays exponentially fast with distance from the wall, it suffices to limit N_c to small integers in order to obtain $\tau(x, y)$ to within machine precision.

3. Results

The resolved shear stress on a slip system with $\theta = \pi/6$ in Eq. (2), due to the two dislocation arrangements shown in Fig. 1 are now presented. The first arrangement, shown in Fig. 1 (a), corresponds to an Archimedean spiral, which obeys the equation $r = D\phi$, where $r = \sqrt{x^2 + y^2}$ and $\phi = \tan^{-1}(y/x)$ represent polar coordinates. D here represents a characteristic dimension, taken to be unity. Dislocations are positioned in the spiral so that the arc length-wise distance between neighbouring dislocations is also D. In the second arrangement, shown in Fig. 1 (b), the dislocations are arranged in a square lattice with lattice constant D. Presently, the resolved shear stresses are computed at the point $(x, y) = (0, D/32)$, assuming $b_{\text{x}}/D = 0$, and $b_{\text{y}}/D = 1$.

Fig. 2 shows the resolved shear stresses computed according to Eq. (5) for various R. With increasing R, $\tau(x, y; R)$ does not approach a limiting value following the scheme of truncated summation, demonstrating the comment following Eq. (5).

Assuming $\varepsilon = 10^{-16}$ in Eq. (7), which is approximately the computer floating point precision, $\tau(x, y; s)$ is computed from Eq. (8), for various $R(s)$. This variation is also shown in Fig. 2, for $s \in \{1/2^0, 1/2^1, \ldots, 1/2^{10}\}$. With decreasing s, $R(s)$ increases. For the spiral arrangement shown in Fig. 2 (a), $\tau(x, y; s)$ is seen to vary non-monotonically for large s, or small $R(s)$. However, for $s \leq 1/2^3$, it increases monotonically and approaches a limiting value. Thus, on one hand, Eq. (8) converges only for $s \leq 1/2^3$ for

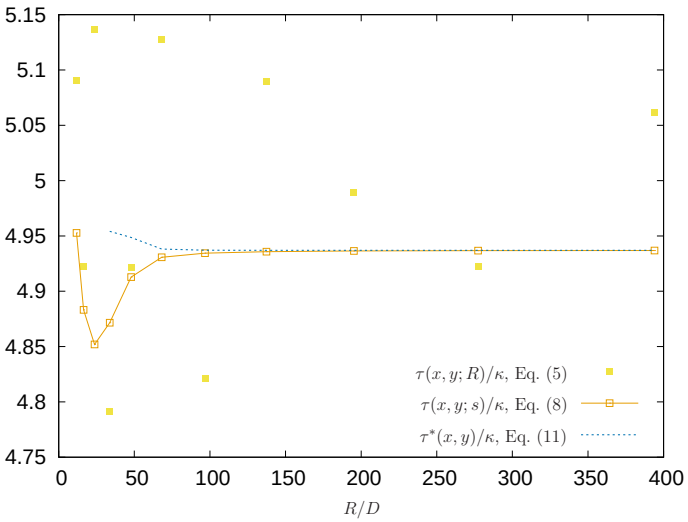

(a) spiral, Fig. 1 (a)

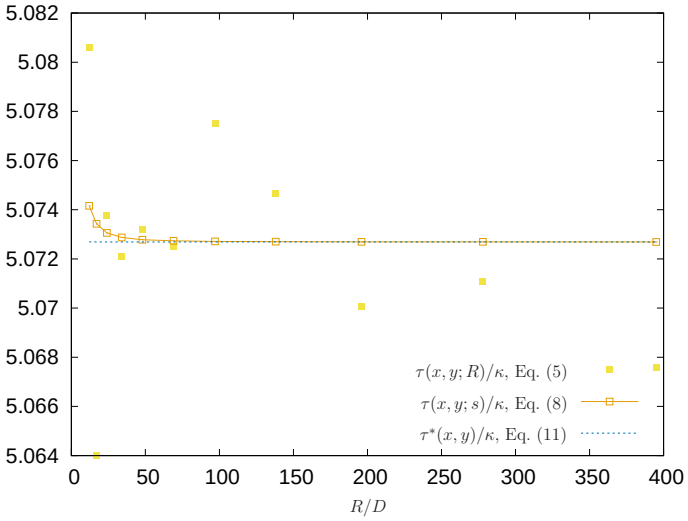

(b) square lattice, Fig. 1 (b)

Figure 2. Resolved shear stress calculated at $(x, y) = (0, D/32)$ using the summation schemes with, and without the convergence factor. The dashed line represents the $s \downarrow 0$ limiting values obtained from Eq. (11) for various $s \in \{1/2^0, 1/2^1, \ldots, 1/2^{10}\}$.

the spiral arrangement, indicating that the domain of summation must be large enough for the summation scheme to 'see' the spiral pattern. On the other hand, for the square lattice, Fig. 2 (b) shows that Eq. (8) converges for $s \leq 1/2^0$, i.e., for all s presently considered.

For both dislocation arrangements, Eq. (10) yields a linear rate of convergence ($p = 1$) for sufficiently small s. Fig. 2 shows the limiting $\tau^*(x, y)/\kappa$ calculated using Eq. (11) as a dashed line for the two arrangements in the asymptotic s-domain of series convergence. Although not evident from the figure, $\tau^*(x, y)/\kappa$ for the spiral arrangement converges to three decimal places at $s = 1/2^6$, and to six decimal places at $s = 1/2^9$. The convergence for the square lattice is much more rapid: Already at $s = 1/2^0$, $\tau^*(x, y)/\kappa$ has converged to six decimal places.

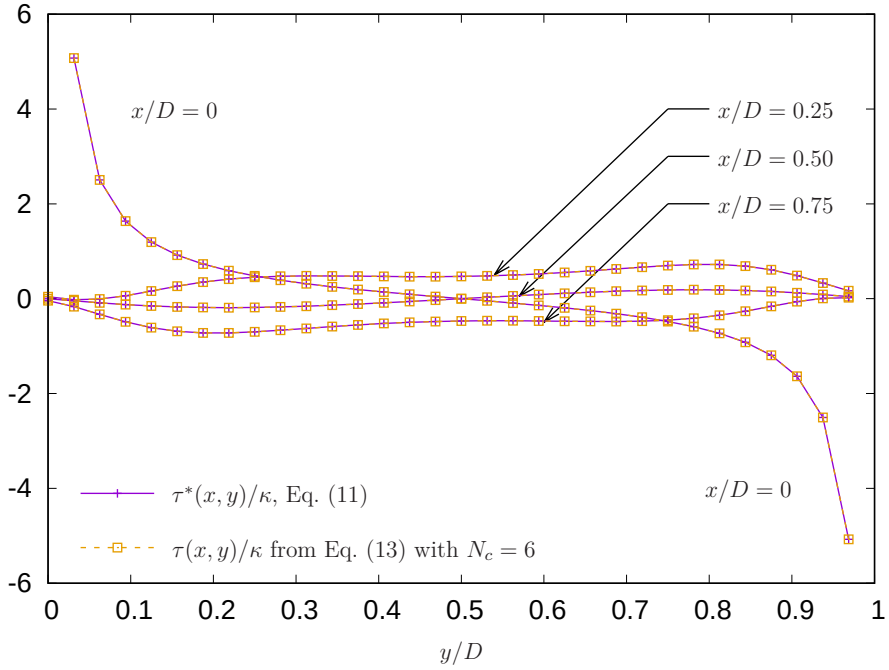

Figure 3. Comparison of the resolved shear stress fields calculated using the present method with those using the method of array summation. Computed resolved shear stresses are shown along four vertical lines, $x/D \in \{0, 1/4, 1/2, 3/4\}$.

Fig. 3 plots the variation of τ^*/κ obtained using the present convergence factor based formula, Eq. (11), and using the array summation formula, Eq. (13), for the dislocation arrangement of Fig. 1 (b). The variations are shown along four vertical lines $x/D \in \{0, 1/4, 1/2, 3/4\}$, $0 \leq y/D \leq 1$. The plots along the $x/D = 0$ line exclude the end points, as the resolved shear stresses there are infinite. It is seen that the resolved shear stresses calculated using the two methods agree exactly. However, the present method offers the advantage of not requiring an explicit correction for the spurious components.

The stress fields corresponding to the square lattice of Fig. 1 (b) satisfy the property $\tau^*(x, y) = -\tau^*(D - x, D - y)$, for $0 \leq x, y \leq D$. This property can be verified in Fig. 3. Therefore, the volume average of $\tau^*(x, y)$ over the region $\{(x, y) : 0 \leq x, y \leq D\}$ is zero.

Consider next, a square lattice of dislocation dipoles, following Gourgiotis and Stupkiewicz [16]. Such a distribution of dislocations may be regarded as two square lattices of single dislocations translated with respect to each other. The Burgers vectors of the dis-

locations in the second lattice are oppositely oriented as those of the first. Let $\tau_1^*(x,y)$, and $\tau_2^*(x,y)$ denote the resolved shear stress fields due to these two lattices, each of which has a zero volume average. The stress field of both lattices is then given by superposition as $\tau_1^*(x,y)+\tau_2^*(x,y)$, which must also have a zero volume average over the region $\{(x,y): 0 \le x,y \le D\}$. This result is consistent with a key finding of Gourgiotis and Stupkiewicz [16].

4. Discussion

A method based on convergence factors has been proposed to compute the stress fields due to an infinite collection of discrete dislocations. The method does not require the dislocations to be grouped into straight arrays, and is thus more general than the array summation method [9, 14–16].

Spurious stresses arise from long-range fields of the set of dislocations. They can be explicitly calculated when they are arranged in a lattice [15], as shown in Fig. 1 (b). But other dislocation arrangements, e.g., Fig. 1 (a) also generate long-range stresses, as a consequence of the eigenstrains associated with the region of summation [16]. In this case, there is no analytical formula for the spurious stress fields. The spurious stresses underlie the non-convergence of summation in Eq. (5), as illustrated in Fig. 2.

The present method assumes that the spurious contribution is of the form cs^p in Eq. (9). In canceling away this term, Richardson extrapolation, Eq. (11), essentially eliminates the spurious contributions to order p. The present method thus eliminates the spurious stresses without explicitly evaluating them.

Summation using the convergence factor only yields a finite solution when the infinite series of Eq. (4) converges. Suppose in Eq. (4), $\tau^O(x-x_i,y-y_i) = C/r_i$, where C is a constant. $\tau^O(x-x_i,y-y_i)$ may then represent the isotropic electrostatic potential of a point charge. If the summation were carried out over the square lattice of Fig. 1 (b), the series is known to diverge [20]. In agreement with this result, Eq. (10) of the present method yields a negative order of convergence, $p=-0.5$, indicating divergence to $\pm\infty$.

Alternately, the infinite series of Eq. (4) may neither converge to a finite value nor diverge to $\pm\infty$. This happens, for instance, when the dislocations of $\mathscr{I}$ are randomly located. In this case, the exponent p in Eq. (10) also fluctuates with s, i.e., it does not approach a limiting value even as $s \downarrow 0$.

5. Conclusion

A fast and simple numerical method is proposed to sum the conditionally convergent series representing the stress fields induced by a two-dimensional countably infinite set of edge dislocations. The method cancels away long range spurious stresses without explicitly evaluating them.

Acknowledgement

The authors gratefully acknowledge funding from the Science and Engineering Research Board (SERB) through sanction order No. PDF/2019/000944.

References

[1] V. Bulatov and W. Cai, *Computer simulations of dislocations*, Oxford University Press, 2006.

[2] L. Kubin, *Dislocations, mesoscale simulations and plastic flow*, Oxford University Press, 2013.

[3] K.M. Davoudi and J.J. Vlassak, *Dislocation evolution during plastic deformation: Equations vs. discrete dislocation dynamics study*, Journal of Applied Physics 123 (2018), p. 085302.

[4] S. Liang, Y. Zhu, M. Huang, and Z. Li, *Simulation on crack propagation vs. crack-tip dislocation emission by XFEM-based DDD scheme*, Int J Plasticity 114 (2019), pp. 87–105.

[5] S. Keralavarma and A. Benzerga, *High-temperature discrete dislocation plasticity*, J Mech Phys Solids 82 (2015), pp. 1–22.

[6] F. Boioli, P. Carrez, P. Cordier, B. Devincre, K. Gouriet, P. Hirel, A. Kraych, and S. Ritterbex, *Pure climb creep mechanism drives flow in earth's lower mantle*, Sci adv 3 (2017), p. e1601958.

[7] R.B. Sills, W.P. Kuykendall, A. Aghaei, and W. Cai, *Fundamentals of dislocation dynamics simulations*, in *Multiscale Materials Modeling for Nanomechanics*, Springer, 2016, pp. 53–87.

[8] L. Greengard and V. Rokhlin, *A fast algorithm for particle simulations*, J Comp Phys 135 (1997), pp. 280–292.

[9] H. Wang and R. LeSar, *$O(N)$ algorithm for dislocation dynamics*, Phil Mag A 71 (1995), pp. 149–164.

[10] R.W. Hockney and J.W. Eastwood, *Computer simulation using particles*, CRC Press, 1988.

[11] D. Barts and A. Carlsson, *Order-N method for force calculation in many-dislocation systems*, Phys Rev E 52 (1995), p. 3195.

[12] J.W. Eastwood, R.W. Hockney, and D. Lawrence, *P3M3DP – the three-dimensional periodic particle-particle/particle-mesh program*, Comp Phys Comm 19 (1980), pp. 215–261.

[13] J.P. Hirth and J. Lothe, *Theory of Dislocations*, Krieger, 1992.

[14] W. Cai, V.V. Bulatob, J. Chang, J. Li, and S. Yip, *Periodic image effects in dislocation modelling*, Phil Mag 83 (2003), pp. 539–567.

[15] W.P. Kuykendall and W. Cai, *Conditional convergence in two-dimensional dislocation dynamics*, Model Simul Mater Sci Eng 21 (2013), p. 055003.

[16] P. Gourgiotis and S. Stupkiewicz, *Macroscopic stress and strain in a doubly periodic array of dislocation dipoles*, Proc R Soc A 470 (2014), p. 20140309.

[17] S.W. de Leeuw, J.W. Perram, and E.R. Smith, *Simulation of electrostatic systems in periodic boundary conditions*, Proc R Soc A 373 (1980), pp. 27–56.

[18] L.F. Richardson and J.A. Gaunt, *The deferred approach to the limit*, Phil Trans R Soc A 226 (1927), pp. 299–361.

[19] G. Birkhoff and G.C. Rota, *Ordinary differential equations*, Ginn, 1962.

[20] S. De Leeuw and J. Perram, *Statistical mechanics of two-dimensional Coulomb systems*, Phys A 113 (1982), pp. 546–558.